EUROFUSION WPS1-CP(16) 15014

N Pablant et al.

Investigation of initial plasma parameters on the Wendelstein 7-X stellarator using the x-ray imaging crystal spectrometer

Preprint of Paper to be submitted for publication in Proceedings of 26th IAEA Fusion Energy Conference

This work has been carried out within the framework of the EUROfusion Consortium and has received funding from the Euratom research and training programme 2014-2018 under grant agreement No 633053. The views and opinions expressed herein do not necessarily reflect those of the European Commission.

Investigation of initial plasma parameters on the Wendelstein 7-X stellarator using the x-ray imaging crystal spectrometer

N. Pablant[1], A. Langenberg[2], O. Marchuk[3], A. Alonso[4], C.D. Beidler[2], S. Bozhenkov[2], M. Bitter[1], L. Delgado-Aparicio[1], G. Fuchert[2], D. Gates[1], J. Geiger[2], K.W. Hill[1], U. Hoefel[2], M. Hirsch[2], J. Knauer[2], A. Krmer-Flecken[3], M. Landreman[7], S. Lazerson[1], H. Maassberg[2], S. Massidda[5], G.H. Neilson[1], E. Pasch[2], J. Svennson[2], P. Traverso[5], Y. Turkin[2], P. Valson[2], J.L. Velasco[4], G. Weir[2], T. Windisch[2], R.C. Wolf[2], M. Yokoyama[6], D. Zhang[2] and the W7-X Team

[1]Princeton Plasma Physics Laboratory
[2]Max-Planck-Institut fur Plasmaphysik
[3]Institut fur Energie- und Klimaforschung, Plasmaphysik, Forschungszentrum Julich
[4]Laboratorio Nacional de Fusion, CIEMAT
[5]Auburn University
[6]National Institute for Fusion Science, Japan
[7]University of Maryland, College Park, MD, USA

Corresponding Author: npablant@pppl.gov

Abstract:

The performance of the Wendelstein 7-X (W7-X) stellarator during the first experimental campaign (OP1.1) is explored using measurements from the x-ray imaging crystal spectrometer (XICS) diagnostic. During OP1.1 plasmas have been produced in a limiter configuration, with up to 4.3 MW of ECH power. The XICS system is designed to provide high-resolution profile measurements of the ion and electron temperatures (T_i, T_e), plasma flow velocity (u), and argon impurity density (n_{Ar}). Profile measurements of T_i and T_e are available with up to 5ms time resolution and 2 cm spatial resolution with coverage of nearly the entire plasma radius. The diagnostic is based on spectroscopic analysis of emission from highly charged Argon impurities that are added to the plasma in trace amounts. Routine measurements from the XICS system are available starting from the first week of W7-X operation. Initial investigations of hydrogen plasmas from the first experimental campaign show thermalized distributions of the ion and electron temperatures. Ion temperatures of $2.2keV$ and electron temperatures in excess of $6keV$ have been achieved in plasmas with $4.3MW$ of ECH heating and electron densities around a few times $10^{-19}m^{-3}$. The detailed evolution of the temperature profiles from these initial plasmas are reported along with initial measurements of argon impurity transport and radial electric field profiles. This collection of plasma measurements, made available by the XICS diagnostic, showcase the versatility and importance of this diagnostic technique.

1 Introduction

The x-ray imaging crystal spectrometer (XICS) diagnostic has played a very important role in machine monitoring and evaluation of plasma performance during the first W7-X experimental campaign (OP1.1). The XICS diagnostic provided the only measurements of the ion temperature (T_i) and central perpendicular flow profiles (u_{perp}) which are invaluable in understanding the plasma performance. This diagnostic was also capable of measuring the density of several charge states of Argon (n_{Ar15+}, n_{Ar16+}, n_{Ar17+}) which are important for the study of impurity confinement. Finally XICS also provided complementary measurements of the electron temperature (T_e) profile which could be compared with the electron cyclotron emission (ECE) and Thomson Scattering diagnostics[1]; the ability to perform multi-diagnostic comparisons was particularly important in providing early confidence in the accuracy of the measured temperature profiles.

2 X-Ray Imaging Crystal Spectrometer

There are two complimentary x-ray imaging crystal spectrometers currently installed on W7-X. The first, XICS, provides coverage over a wide range of the plasma cross-section, and has two fixed channels to measure the Ar^{16+} (He-like) and Ar^{17+} (H-like) emission spectra. Routine measurements from the Ar^{16+} channel are available starting from the first week of W7-X operation; the second channel is expected to be in operation for the next W7-X campaign (OP1.2). The second system, HR-XIS (High Resolution X-Ray Imaging Spectrometer), provides more limited spatial coverage but can be remotely tuned to view a wide range of emission spectra in the soft x-ray range (around 3Å). Data from the HR-XIS system was only available during the last week of the OP1.1 campaign. The current paper will focus on the results from the XICS diagnostic, however the basic principles and capabilities are similar between the two systems. Detailed descriptions of the XICS and HR-XICS diagnostics can be found in Ref. 2 and Ref. 3 and the diagnostic concept has been explained in detail by Bitter *et al.* in Ref. 4.

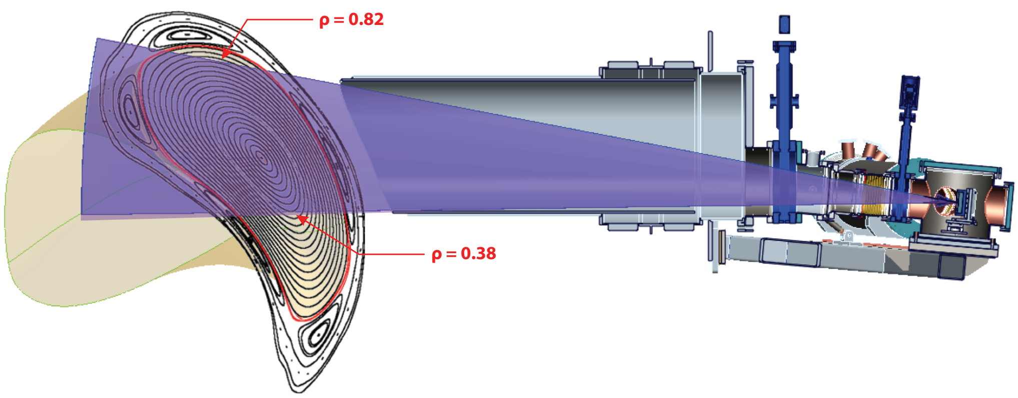

FIG. 1: Viewing geometry of the the XICS diagnostic on W7-X.

The XICS diagnostic is based on spectroscopic analysis of emission from highly charged argon impurities that are added to the plasma in trace amounts[4]. The XICS system records a 1D image of line integrated spectra. These line integrated signals can be used to find local plasma parameters by utilizing tomographic inversion techniques with a known equilibrium [5, 6]. Standard Doppler spectroscopy techniques are used to extract information from the recorded spectra: Ion temperatures (T_i) are found from the line widths, electron temperatures (T_e) from line ratios, plasma flow (u) from the line shifts, and impurity densities ($n_{Ar^{15+/16+/17+}}$) from the line amplitudes[4].

An additional analysis technique is also in development which utilizes the `MINERVA`[7] framework and a complete forward model to determine the local plasma parameters from the raw line integrated images[8]. This Bayesian technique is expected to result in the most accurate deduction of the plasma parameters, however it has a cost of being slow to compute. A distinct advantage of using `MINERVA` for analysis is that in principle multiple diagnostics can be added to the analysis to provide an overall most consistent set of plasma profiles. Details of XICS analysis using `MINERVA` along with current results are given in these proceedings in Ref. 9.

For typical W7-X discharges argon puffing is introduced to achieve an argon density fractions of $\approx 10^{-4} n_{Ar}/n_e$. Dedicated experiments with and without puffing have demonstrated that at these levels the injected argon has no measurable effect on plasma performance. Argon puffing is done either using the standard gas injection system, or using the He-beam diagnostic[10]. For most W7-X discharges the argon is introduced during the 'prefill' phase, before ECH heating begins, however injection during a discharge is also effective and can used both to study impurity transport and to maintain a minimum argon level during long discharges.

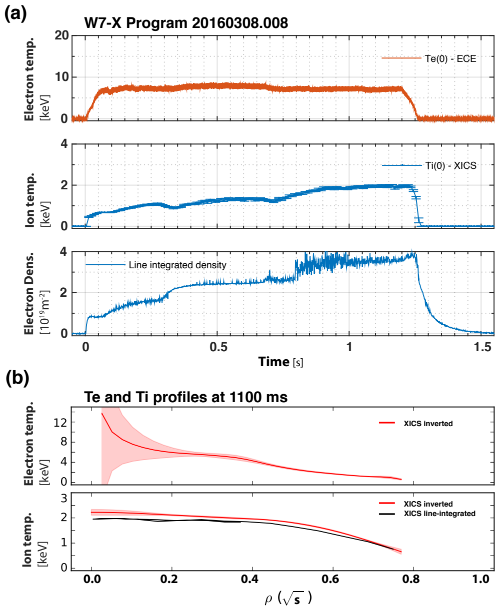

FIG. 2: Evolution of ion temperature as measured by XICS. In Fig (a) the Central ion temperature from line integrated XICS analysis is shown. In Fig (b) inverted T_e and T_i profiles are shown for the peak ion temperature at $1100ms$.

The XICS hardware allows profile measurements with up to 5ms time resolution and 2 cm spatial resolution with coverage of nearly the entire plasma radius (see Fig.1). Ion and electron temperature profiles are achievable at this resolution with the standard argon puffing levels with accuracies in the range of $10eV$ and $100eV$ respectively. With smaller amounts of argon puffing (less argon emissivity) longer integration times or more spatial binning of the data is necessary to achieve high quality measurements. Flow velocity measurements can generally be made with temporal and spatial resolutions of $10ms$ and $2cm$ respectively and an accuracy of $\approx 1km/s$, which corresponds to a line shift of $0.01m\text{Å}$ ($0.025pixels$), and ultimately to accuracy in E_r of $\approx 2.5kV/m$.

3 Ion temperature

During OP1.1 XICS was the only diagnostic that could provide ion temperature measurements. While XICS measures the temperature of the argon atoms, at typical plasma densities of a few times $10^{19}m^{-3}$ it is expected that the impurity ions would be thermally equilibrated with the main ions. Heating during this first experimental phase was purely through electron cyclotron resonance heating (ECRH) with $4.3MW$ of available power; the only source of heating for the ions was through collisional heat transfer from the electrons.

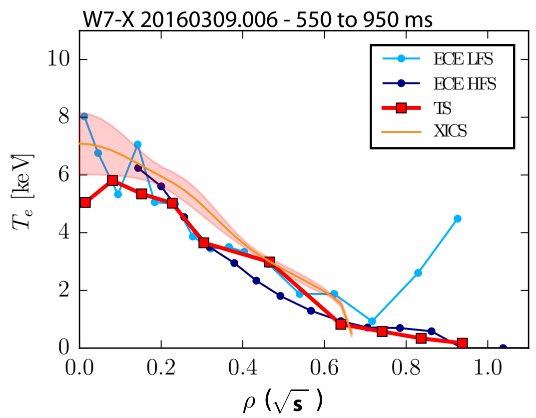

FIG. 3: Comparison of electron temperature profiles from XICS (inverted), Thomson Scattering and ECE.

The ability to measure T_i profiles has allowed the initial performance of W7-X to be evaluated. Ion temperature profiles, in conjunction with measurements of the electron density and temperature, have allowed the kinetic stored energy to be estimated and compared with measurements by the diamagnetic loop[11]. These two methods of determining the stored energy agree very well for most plasmas, which provides confidence that both that the electron and ion temperatures are thermalized. Simple power balance calculations based on the heating, temperature profiles and radiated power allow estimates of the confinement time to be calculated. The estimated confinement time from these considerations is typically found to be around $100 - 150ms$[11, 12], which is also consistent with the decay of the stored energy after plasma heating is terminated.

The highest recorded ion temperature during OP1.1 was achieved through a series of density steps in a high power plasma[13]. The final equilibrium temperatures achieved with $4.3MW$ of ECRH power were $T_{io} = 2.2keV$ and $T_{eo} = 6keV$ with a line integrated density of $\overline{n_e} = 4 \times 10^{19}m^{-2}$ as shown in Fig.3. In these purely ECRH heated plasmas, higher ion temperatures would require higher densities, which were not achievable in OP1.1 due to impurity radiation becoming unsustainable with increasing density. This is expected to be much improved during OP1.2 which will be diverted rather than limited and have better wall conditions.

4 Electron temperature

During the first experimental campaign routine measurements of the electron temperature profile were available through three diagnostics: electron cyclotron emission (ECE)[14], Thomson scattering[1] and XICS. These three diagnostics use entirely different techniques for the determination of T_e and therefore provide an excellent means of validating the measurements. This was of particular importance during the first days of the campaign where the quality of the calibration of each diagnostic was still being evaluated. In the majority of cases all three diagnostics provide identical measurements of T_e, within the expected error bars. This matching of the diagnostic measurements also provides a strong indication that the electrons are thermal as each diagnostic would be expected to react to non-thermal distributions in different ways.

While the XICS is able to make measurements of the T_e profile, it is poorly suited to measuring the central electron temperature profile in typical OP1.1 plasmas. The T_e measurement is based on the ratio of lines within the Ar^{16+} spectrum, in particular the ratio of the resonance line to the dielectronic satellite lines[15]. To obtain the inverted (local) electron temperature each of the line intensity profiles is independently inverted, then the ratio of the inverted emissivity profiles is used to determine T_e. When the electron temperatures exceeds $\sim 3keV$ the intensity of the dielectronic satellite greatly decreases along with the the total fraction of argon atoms in the Ar^{16+} ionization state. This leads to the dielectronic satellite emissivity profile to be very hollow, a case where the uncertainty in the inversion process can be very large (as seen in Fig.2 and Fig.3). This is compounded by the line ratio becoming increasingly insensitive to changes in the electron temperature. The end result is that while the XICS can make high quality T_e measurements in colder regions of the plasma, the technique has large uncertainties in the hot plasma core as seen in Fig.3.

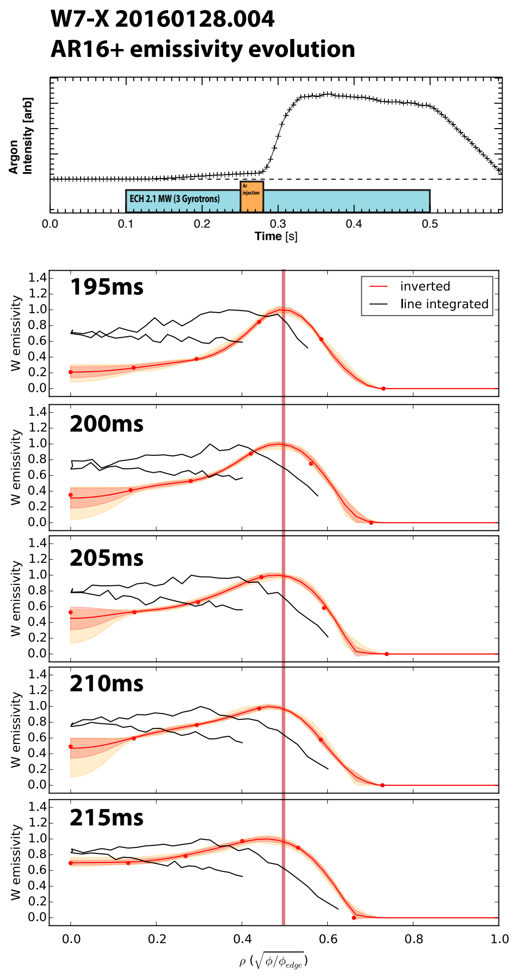

FIG. 4: Argon transport experiments utilizing fast gas puffs. Argon is injected at 250*ms from the He-Beam gas injector. A slow decay in the argon intensity is seen in the later portion of this discharge. Plasma parameters (T_e, n_e, T_i are constant after* 150*ms.*

This situation is expected to improve dramatically in OP1.2 for two reasons: First at higher densities the electrons will be better equilibrated with the ions, and therefore T_e will be lower at equivalent input power. Secondly quality XICS measurements will be possible at higher temperatures due to the addition of an Ar^{17+}/Fe^{24+} channel for the XICS system, and the installation of multiple crystals in the HR-XIS system that allow analysis of emission from a variety of impurities.

5 Argon impurity density

Impurity transport is another topic in which the XICS has played an important role. XICS is the only diagnostic that was able to provide density profiles of any impurity species during OP1.1. In particular XICS is able to directly measure the density profile for the Ar^{15+} and Ar^{16+} charge states, and to infer the Ar^{17} density profile though line ratios based on recombination[9, 16]. The complementary system HR-XIS was also tuned to directly measure the Ar^{17} density profile[16]. In addition the High Efficiency XUV Overview Spectrometer (HEXOS) can measure line integrated intensities of lower charge states of argon down to Ar^{6+}[17]. These three diagnostics together provide a very detailed coverage of argon charge state density profiles and temporal evolution.

A set of experiments was carried out in which a short puff of argon ($20ms$) was injected using the He-Beam diagnostic[10] during the flat top phase of a discharge (see Fig.4). These experiments allow the study of argon inward transport by looking at the rise time of the argon emissivity after the gas puff as well as the global impurity confinement by observing the decay in the argon emissivity in later portions of the discharge. Initial investigations put the global argon confinement time at $200 - 300ms$, but do not include a full treatment of the effects of recycling. The initial rise of argon emissivity is discussed by Ref. 9 in these proceedings.

6 Radial Electric Field

In stellarator plasmas the neoclassical particle fluxes are not intrinsically ambipolar, which leads to the formation of a radial electric field that (E_r) enforces ambipolarity. The details of the Er profile are expected to have a strong effect on both the particle and heat fluxes as well as the bootstrap current [18, 19]. For the plasma conditions seen during the OP1.1 campaign, which feature centrally peaked electron temperature profiles and $T_e \gg T_i$, the formation of a positive radial electric field (electron-root) in the plasma core is expected as seen on other stellarator devices[20]. The study of the core positive radial electric field plasmas was an important part of the OP1.1 experimental campaign[19].

The XICS system is able to measure plasma flows along the direction of the sightlines, and is primarily sensitive to the component of the velocity that is perpendicular to the magnetic field. These perpendicular plasma flow profiles are closely related to the radial electric field through the force balance equation and allow routine estimations of E_r on W7-X[21].

These initial estimates of E_r from the XICS diagnostic show that a positive radial electric field (electron-root) is seen in the core of the plasma in all analyzed plasmas in OP1.1. The precise shape and magnitude of the E_r profile changes along with the specific heating power and plasma profiles as seen in Fig.5. These measurements have been compared to neoclassical calculations using the SFINCS[22] and DKES[23] codes, and show excellent agreement both in general shape, radius of cross over from positive (electron-root) to negative (ion-root) field, and general magnitude. This first experimental validation of neoclassical predictions provides additional confidence in the validity of neoclassical theory

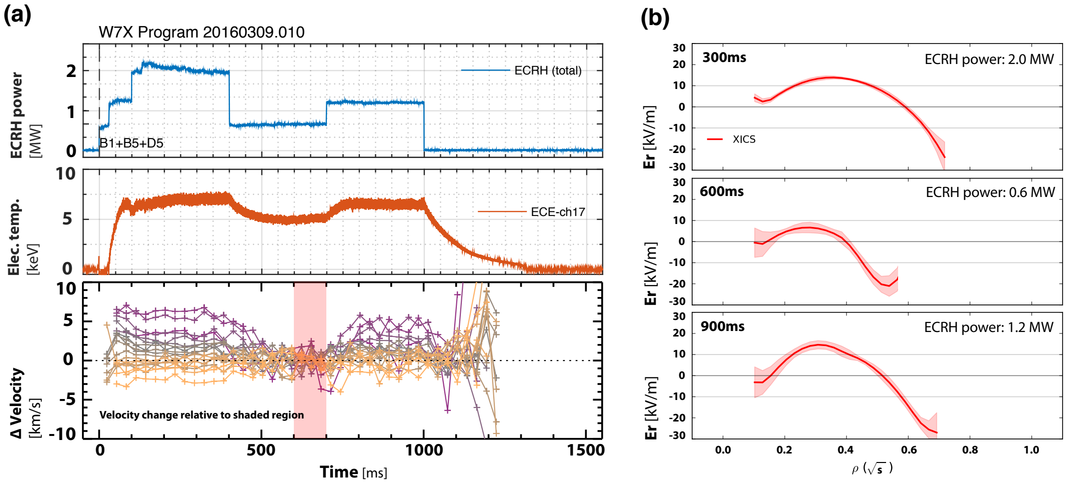

FIG. 5: Fig (a): Dynamic evolution of the plasma flow as measured by XICS. For clarity, the change in velocity seen in individual XICS sightlines is shown relative to the value at 650 ms. Purple and yellow lines represent views above and below the magnetic axis respectively. Fig (b): Radial electric field profiles inferred from XICS flow velocity measurements.

and the simplifications used in the computational code for the W7-X configuration[19, 21].

The detailed shape of the E_r profile, either from XICS or from validated neoclassical predictions, will play an important role in understanding much of the detailed core heat and particle transport in W7-X plasmas. An example is the addition of E_r into impurity transport codes coupled with neoclassical particle transport calculations.

7 conclusion

The x-ray imaging crystal spectrometer diagnostic has played a crucial role during the first W7-X experimental campaign. It has been instrumental in understanding the plasma ion and electron temperature profiles, plasma confinement and overall performance, impurity transport, the role of the radial electric field, and in experimental validation of neoclassical predictions. The ability to make these measurements with good spatial and time resolution using only non-perturbative levels of trace argon injection has also been demonstrated. The wide range of high quality profile measurements available using a single, relatively simple diagnostic, along with the maturity of available analysis packages, make XICS a highly desirable diagnostic for current and future stellarator devices.

Research supported by the U.S. DOE under Contract No. DE-AC02-09CH11466 with Princeton University. This work has been carried out within the framework of the EUROfusion Consortium and has received funding from the Euratom research and training programme 2014-2018 under grant agreement No 633053. The views and opinions expressed herein do not necessarily reflect those of the European Commission.

References

[1] *PASCH, E. et al., 43rd EPS Conference on Plasma Physics (2016) P4.016.*

[2] *PABLANT, N. et al., Europhysics Conference Abstracts* **38F** *(2014) P1.076.*

[3] *LANGENBERG, A. et al., 41st EPS Conference on Plasma Physics (2014).*

[4] *BITTER, M. et al., Review of Scientific Instruments* **81** *(2010) 10E328.*

[5] *PABLANT, N. A. et al., Plasma Physics and Controlled Fusion* **58** *(2016) 045004.*

[6] *PABLANT, N. A. et al., Review of Scientific Instruments* **85** *(2014) 11E424.*

[7] *SVENSSON, J. et al., IEEE International Symp. on Intelligent Signal Processing (2007).*

[8] *LANGENBERG, A. et al., Fusion Science and Technology* **69** *(2016) 560.*

[9] *LANGENBERG, A. et al., Proceedings of the 26th IAEA Fusion Energy Conference (2016) EX/P5.*

[10] *BARBUI, T. et al., Review of Scientific Instruments* **87** *(2016) 000000, accepted for publication.*

[11] *BOZHENKOV, S. et al., 43rd EPS Conference on Plasma Physics (2016) O2.106.*

[12] *HIRSCH, M. et al., Proceedings of the 26th IAEA Fusion Energy Conference (2016) EX/4.*

[13] *KÖNIG, R. et al., 43rd EPS Conference on Plasma Physics (2016) I2.108.*

[14] *HIRSCH, M. et al., 43rd EPS Conference on Plasma Physics (2016) P4.007.*

[15] *MARCHUK, O.,* Modeling of He-like spectra measured at the tokamaks TEXTOR and TORE SUPRA*, PhD thesis, Ruhr-Universität Bochum, 2004.*

[16] *LANGENBERG, A. et al., 43rd EPS Conference on Plasma Physics (2016) P4.014.*

[17] *BUTTENSCHÖN, B. et al., 43rd EPS Conference on Plasma Physics (2016) P4.012.*

[18] *MAASSBERG, H. et al., Physics of Plasmas* **16** *(2009).*

[19] *DINKLAGE, A. et al., 43rd EPS Conference on Plasma Physics (2016) O2.107.*

[20] *YOKOYAMA, M. et al., Nuclear Fusion* **47** *(2007) 1213.*

[21] *PABLANT, N. et al., 43rd EPS Conference on Plasma Physics (2016) P4.013.*

[22] *LANDREMAN, M. et al., Physics of Plasmas* **21** *(2014).*

[23] *VAN RIJ, W. I. et al., Physics of Fluids B* **1** *(1989) 563.*